

^{18}F -FDG PET imaging of progressive massive fibrosis

Soo Yoon Chung · Jae Hoon Lee · Tae Hoon Kim ·
Sang Jin Kim · Hyung Joong Kim · Young Hoon Ryu

Received: 22 February 2009 / Accepted: 28 October 2009 / Published online: 25 November 2009
© The Japanese Society of Nuclear Medicine 2009

Abstract

Purpose This study was to evaluate ^{18}F -FDG PET features of progressive massive fibrosis (PMF) and to determine the ability of FDG PET to differentiate pure PMF from PMF-associated lung cancer.

Methods ^{18}F -FDG PET and chest computed tomography (CT) scans were performed in 9 patients with pneumoconiosis and PMF. Patients who showed active pulmonary tuberculosis on CT scan were excluded. Pure PMF was confirmed via either fine needle aspiration biopsy ($n = 6$) or 12 months follow-up CT scan ($n = 3$). CT features and PET findings were evaluated for distribution of fibrotic masses, consolidations, and nodules on CT scan and mean and maximum standardized uptake values (SUVs) of abnormalities depicted on PET scan.

Results 14 masses were detected from nine patients. On chest CT scan, PMF masses were noted with surrounding small nodules and distortion of parenchyma. The size of the lesions ranged from 1.2 to 6.4 cm in maximum diameter. FDG PET scans identified metabolically active lesions in all patients. Maximal SUV ranged from 3.1 to 14.6 and mean SUV ranged from 1.4 to 8.5.

Conclusion FDG PET can identify PMF lesions as hypermetabolic lesions even without associated malignancy or tuberculosis. Therefore, it might have a limited role in the diagnosis of PMF with possible concurrent granulomatous inflammation or lung cancer.

Keywords Progressive massive fibrosis · Pneumoconiosis · Lung cancer · ^{18}F -FDG PET · Chest CT

S. Y. Chung
Department of Diagnostic Radiology, Yongin Severance Hospital, Research Institute of Radiological Science, Yonsei University College of Medicine, Yongin, Kyunggi-Do, Republic of Korea

J. H. Lee · T. H. Kim · S. J. Kim
Department of Diagnostic Radiology, Gangnam Severance Hospital, Yonsei University College of Medicine, Seoul, Republic of Korea

H. J. Kim
Department of Pulmonology, Gangnam Severance Hospital, Yonsei University College of Medicine, Seoul, Republic of Korea

Y. H. Ryu (✉)
Division of Nuclear Medicine, Department of Diagnostic Radiology, Gangnam Severance Hospital, Research Institute of Radiological Science, Yonsei University College of Medicine, 146-92 Dogok-Dong, Kangnam-Gu, Seoul 135-270, Republic of Korea
e-mail: ryuyh@yuhs.ac

Introduction

Progressive massive fibrosis (PMF) of the lung occurs in patients with a history of pneumoconiosis and is defined as a fibrotic lesion usually greater than 1 cm in diameter [1]. PMF lesions tend to rapidly increase in size, and the patients have an increased risk of tuberculosis and lung cancer. The lesion commonly involves the apical and posterior segments of the upper lobes and may cross the interlobar fissures into the adjacent lobe [2, 3]. The radiographic and computed tomography (CT) findings have been well documented [3–5]; however, PMF is occasionally difficult to distinguish from lung cancer radiologically as well as clinically, especially when considering the high incidence of lung cancer in PMF patients [6–8]. Although CT scans have a high rate of sensitivity for the detection of pulmonary nodules and masses, the nature of PMF lesions

is difficult to characterize, and observation or a more invasive diagnostic approach, such as biopsy, is needed to determine whether the lesions are malignant or benign [9, 10].

Currently in nuclear medicine, ^{18}F -2-fluoro-2-deoxyglucose positron emission tomography (^{18}F -FDG PET) is widely used as a method for the detection and staging of almost all tumors in any region of the body [11, 12]. The ability of PET imaging using ^{18}F -FDG to exploit the biochemical differences between normal and neoplastic tissue has resulted in its wide use for characterizing lesions that are indeterminate by conventional imaging modalities.

Recently, a few case reports documented successful diagnostic results in detecting lung cancer arising from PMF associated with pneumoconiosis [13, 14]. However, to the best of our knowledge, only limited data on the PET appearance of PMF have been documented [15, 16], and even less on the diagnostic value in distinguishing associated lung cancer from pure PMF.

The purpose of this study was to evaluate the ^{18}F -FDG PET features of PMF and to determine the ability of ^{18}F -FDG PET to differentiate pure PMF from PMF-associated lung cancer.

Materials and methods

Patient selection

We retrospectively reviewed the patients with pneumoconiosis from February 2001 to December 2006. All patients who showed PMF on plain chest X-ray underwent chest CT scan and ^{18}F -FDG PET. Those who showed any evidence of active pulmonary tuberculosis on high-resolution CT scan were excluded in this study. The institutional review board at Gangnam Severance hospital approved the study.

The database consisted of seven male and two female patients (mean age 58.8 ± 6.3 years, range 48–72). Of the nine patients, six patients underwent CT-guided fine needle aspiration biopsies targeted to the area of highest FDG uptake, and the other three patients had a 12-month follow-up chest CT scan.

Chest CT scan protocol

Chest CT scans were performed using a 16-channel multi-detector row CT scanner (Somatom Sensation 16, software version VA20, Siemens Medical Solutions, Forchheim, Germany) with a 6-mm collimation and a 6-mm reconstruction interval. The exposure parameters for the CT scans were 120 kVp and 250 mAs. In all patients, non-contrast CT scans were obtained at the level of the lesion. A total of 100 ml of Iopromide (Ultravist 300; Bayer Schering Pharma, Leverkusen, Germany) were administered intravenously at a rate of 3 ml/s for postcontrast CT scan. HRCT scans were also obtained throughout the thorax (1.0-mm collimation at 10-mm intervals; scans obtained at end inspiration).

PET protocol

All consecutive patients underwent FDG PET scanning after PMF was verified on CT scans with a whole-body tomography scanner (Allegra, Philips, Eindhoven, Netherlands). This scanner provided a 57.6 cm axial field of view and 18.5 cm transaxial field of view, which produced 46 image planes, spaced 4.02 mm apart. Transaxial spatial resolution was 4.2 mm full-width at half-maximum (FWHM) at the center of the field of view, and axial resolution was 5.0 mm FWHM. Patients fasted for at least 6 h before intravenous injection of 370 MBq ^{18}F -FDG, and the mean serum glucose level was 93 mg/dl (range 63–122)

Table 1 Demographic data and results of chest CT, F-18 FDG PET, FNAB, and follow-up CT

Case no.	Age	Sex	CT findings of PMF			SUV of F-18 FDG		Result of further evaluation	
			Size (cm) ^a	Lobar distribution	Laterality	Peak	Mean	Procedure	Result
1	76	M	3.3/3.0	Upper	Bilateral	5.2/4.3	3.4/2.1	CT-guided FNAB	Negative for malignancy
2	56	M	5.3/1.7	Upper	Bilateral	5.9/7.2	3.1/3.7	CT-guided FNAB	Negative for malignancy
3	48	M	5.5	Upper	Lt.	9.2	6.4	CT-guided FNAB	Negative for malignancy
4	63	M	5.1/3.9	Upper	Bilateral	6.8/4.1	4.9/1.5	CT-guided FNAB	Negative for malignancy
5	49	F	4.1	Upper	Rt.	4.4	2.9	CT-guided FNAB	Negative for malignancy
6	61	M	5.3/5.0	Upper	Bilateral	14.6/10.2	8.5/4.0	CT-guided FNAB	Negative for malignancy
7	68	M	6.4	Upper	Rt.	7.3	3.5	12-month follow-up CT scan	No interval change
8	55	F	2.5/2.0	Upper	Bilateral	4.8/3.1	3.0/1.4	12-month follow-up CT scan	No interval change
9	52	M	1.2	Upper	Lt.	4.5	4.3	12-month follow-up CT scan	No interval change

FNAB fine needle aspiration biopsy

^a In the cases with bilateral masses, the first values represent the larger masses, regardless of involved side and FDG uptakes

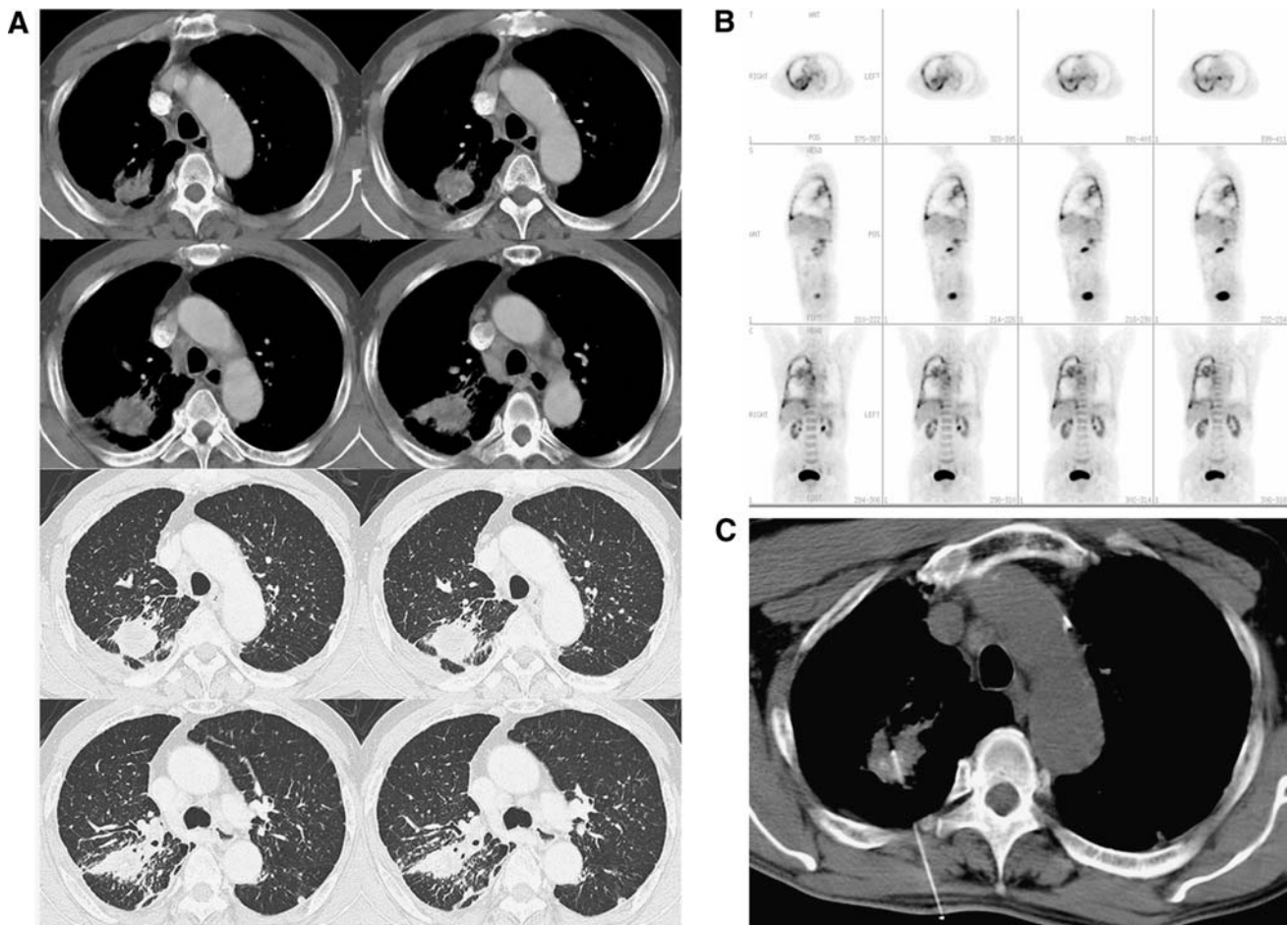


Fig. 1 48-year-old male with PMF. **a** Postcontrast CT and HRCT shows round, ill-defined mass in the right upper lung. **b** PET images show increased uptake of the mass and diffuse pleural uptake of right

thorax. **c** CT-guided percutaneous biopsy was performed, and proved as negative for malignancy

just before injection. Whole-body emission scans were obtained in all patients 40–60 min after injection using multiple bed position techniques. Seven to eight bed positions from the external acoustic meatus to the thigh were imaged for 4 min per bed position. All patients were studied in the supine position with their arms raised. Attenuation-corrected transaxial images were reconstructed with an iterative transmission algorithm called RAMLA (Row-Action Maximum-Likelihood) 3D protocol using 3D image filter into a 128×128 matrix.

Image interpretation

All CT scans were analyzed by two chest radiologists. As seen on CT scan, patterns of parenchymal abnormalities were thoroughly evaluated for the distribution of fibrotic masses, consolidations, and surrounding small nodules. Each lesion was measured in its longest dimension on the axial plane. Lobar distribution and laterality (unilateral or bilateral) of each lesion were evaluated.

Two experienced, independent investigators, who were blinded to the clinical data and results of CT scans, interpreted the PET images. ^{18}F -FDG PET findings were meticulously evaluated for the distribution of masses, consolidations, and nodules on the CT scans, and maximal and mean standardized uptake values (SUVs) of abnormalities depicted on the F-18 FDG PET scans. Lesions were identified and subjectively characterized in relation to normal anatomy and surrounding tissue uptake. For semi-quantitative evaluation of ^{18}F -FDG uptakes, ROIs were defined around suspicious ^{18}F -FDG accumulations in transaxial slices. The maximum counts in a selected ROI were chosen for the calculation of maximal SUV.

Further evaluation

In six patients, CT-guided aspiration biopsies using 22G fine needles were performed from the masses targeted to the area of highest FDG uptake. Cytology was reviewed by an experienced lung pathologist. The other three patients

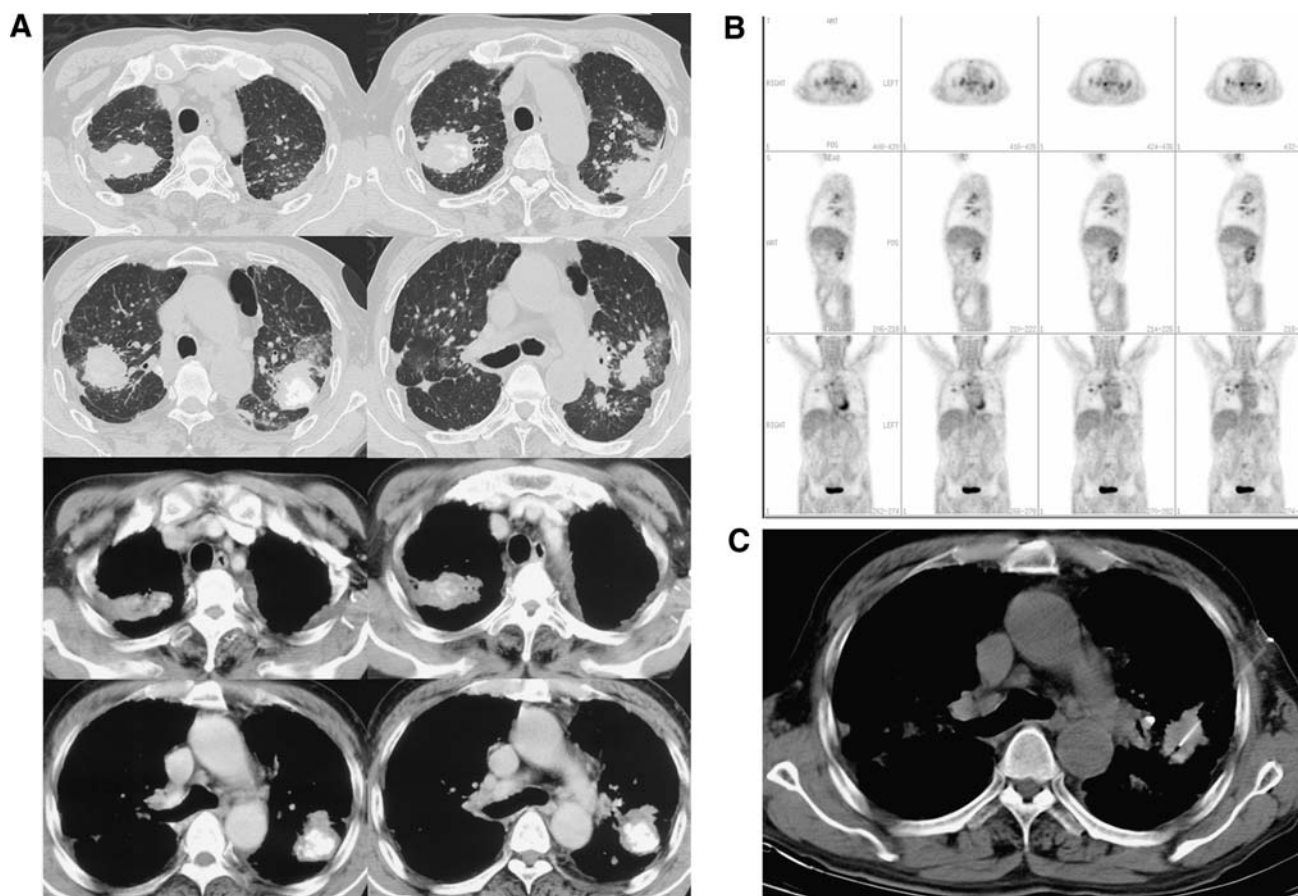


Fig. 2 63-year-old male with PMF. **a** CT scans show bilateral upper lung fibrotic masses with surrounding small nodules. **b** High FDG uptakes are observed in both masses on PET scan. **c** CT-guided FNAB was performed in the left lung mass, and proved as negative for malignancy

underwent 12-month follow-up CT scans for interval changes to exclude the possibility of a combined lesion such as cancer or infection.

Results

Chest CT findings

14 masses were detected from nine patients. Demographic data and radiographic findings are summarized in Table 1. On initial chest CT scan, all patients demonstrated upper lung fibrotic masses with surrounding small nodules (Figs. 1a, 2a, 3a). Unilateral mass was found in four patients and bilateral mass lesions in six patients. The mean size of the masses, which was the greatest diameter measured on trans-axial HRCT images, was 3.9 ± 1.6 cm (range 1.2–6.4 cm).

^{18}F -FDG PET findings

As illustrated in the following figures (Fig. 1b, 2b, 3b), high FDG uptakes by individual masses were depicted on PET scans. The maximal SUV ranged from 3.1 to 14.6 with

a mean value of 6.5 ± 3.1 . The mean SUV ranged from 1.4 to 8.5 with a mean value of 3.8 ± 1.9 .

Further diagnostic procedures

Fine needle aspiration biopsy (FNAB)

Computed tomographic-guided percutaneous FNAB was performed in six patients (Fig. 1c, 2c); three patients showed increases in mass size on follow-up chest radiographs, while the other three patients had atypical PMF configurations, which were spherical rather than spindle-shaped, irregular with ill-defined lateral borders, and not parallel to the major fissure. In correlation with maximal ^{18}F -FDG uptake foci, CT-guided percutaneous biopsy taken with a 22G fine needle was performed. Cytology consistently revealed abundant inflammatory cells and fibrosis without any evidence of malignancy.

Follow-up chest CT scans

The other three patients underwent 12-month follow-up CT scans for the evaluation of interval changes. Follow-up CT

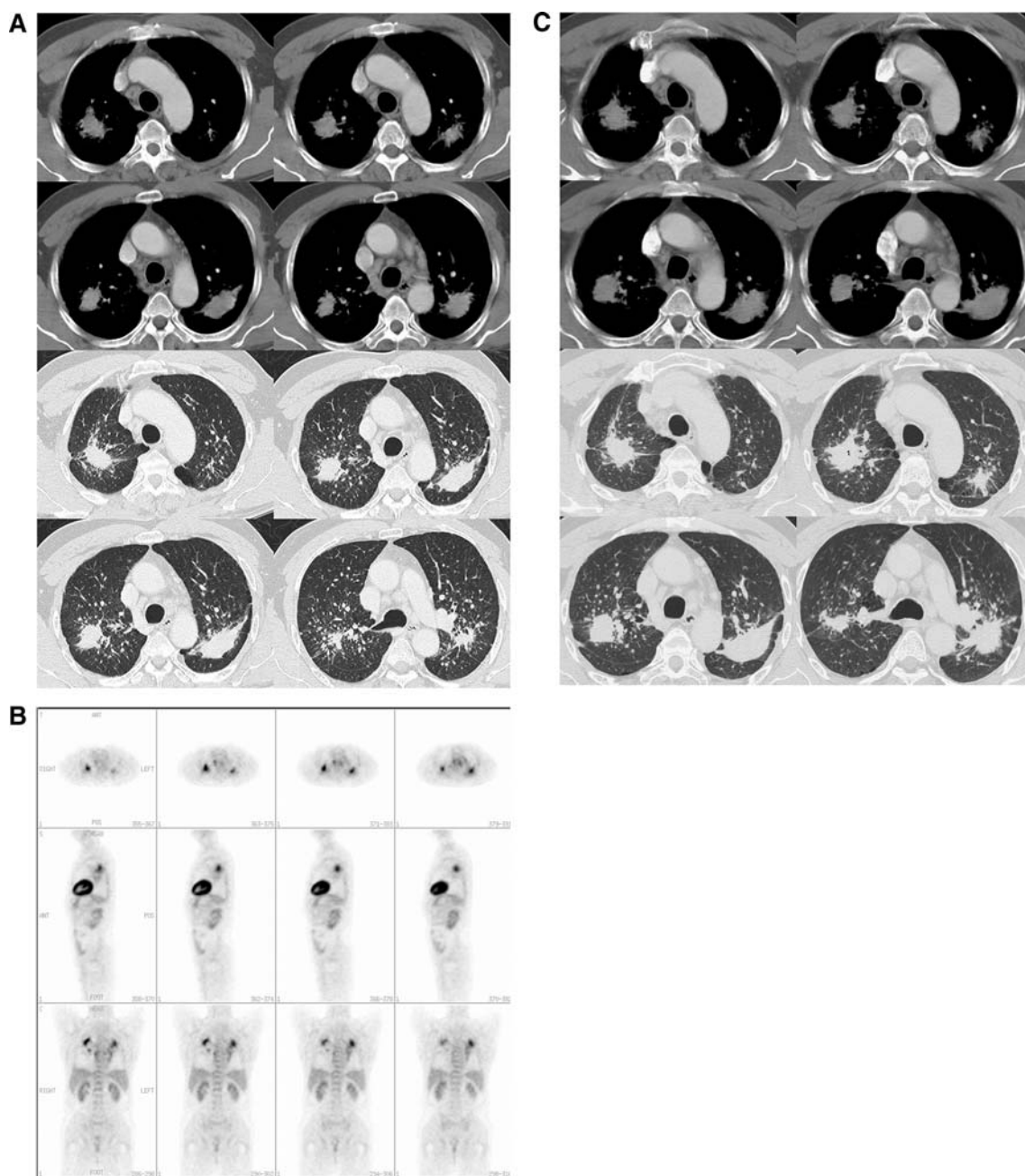


Fig. 3 68-year-old male with PMF. **a** Initial CT scan shows bilateral upper lung fibrotic masses with surrounding small nodules. **b** High FDG uptakes are noted in both masses on PET scan. **c** 12-month follow-up CT scan shows no remarkable interval changes in bilateral mass lesions

scans showed no remarkable interval changes in size or configuration of the masses in these patients (Fig. 3c).

Discussion

Progressive massive fibrosis is defined as a lesion of fibrosis and pigment deposition larger than 1 cm in diameter and is sometimes diagnosed as complicated pneumoconiosis. These lesions commonly occur in coal workers

who have had exposure to heavy dust and who show a large amount of dust in the lungs at autopsy [1, 2]. Radiologically, PMF starts near the periphery of the lung and appears as a mass with a smooth, well-defined lateral border that parallels the rib cage. In contrast to its sharp lateral border, the medial margin of the mass is often ill defined. It tends to be thicker in the coronal than in the sagittal plane, appearing as a broad opacity on frontal radiograph and thin on the lateral projection, frequently paralleling the major fissure [3].

Although typical CT features of PMF have been well documented, a large homogeneous mass of PMF in the parahilar lung may closely resemble pulmonary carcinoma [17]. In this situation, the presence of additional radiographic evidence of pneumoconiosis may suggest a diagnosis of PMF; however, when PMF is unassociated with such radiographic evidence, the differential diagnosis is very difficult [18]. In addition, even with other radiographic features of pneumoconiosis, the differential diagnosis of pure PMF, which is not associated with lung cancer, may be of great clinical importance. High incidence of lung cancer has been reported in patients with pneumoconiosis either with or without PMF. Additionally, Katabami et al. [19] suggested that pneumoconiosis-associated diffuse fibrosis may accelerate the progression of lung cancer, especially peripheral-type squamous cell carcinomas. Therefore, pneumoconiosis-associated diffuse fibrosis should be carefully followed for early detection of lung cancer. Recently, studies on magnetic resonance imaging (MRI) signal characteristics of PMF have been published; however, the diagnostic value of MRI in the accurate differentiation of PMF from malignancy or inflammatory lesions has not yet been well established [17, 20, 21]. To the best of our knowledge, only a few case reports have been published about F-18 FDG PET findings of PMF. Bandoh et al. [13] and Je et al. [14] reported successful delineation of lung cancer associated with PMF using F-18 FDG PET scans, thus demonstrating a potential role of ^{18}F -FDG PET scans in detection of lung cancer in patients with pneumoconiosis.

In our study, all of our cases showed abnormal uptake of ^{18}F -FDG, and the uptake areas corresponded to PMF on chest CT scans; maximal SUV ranged from 3.1 to 14.6 and mean SUV ranged from 1.4 to 8.5. Measured values were equivalent to those of cancerous conditions. However, results from our ^{18}F -FDG PET scans were proven to be false positives by CT-guided percutaneous biopsies ($n = 6$) and 12-month follow-up studies ($n = 3$). As a result, the use of ^{18}F -FDG PET was limited in the differential diagnosis of pure PMF from lung malignancy or from PMF-associated lung cancer.

FDG PET scans have previously been thought to be able to exploit the metabolic differences between PMF and lung cancer; however, false positive FDG PET results in patients with pneumoconiosis have been reported in the literature [16, 22]. Microscopically, PMF shows bundles of haphazardly arranged, sometimes hyalinized bands of collagen interspersed with numerous pigment-laden macrophages and abundant-free pigment in the central regions, with destruction of surrounding tissue and a variable degree of expanding fibrotic processes [23]. On the basis of pathology, pure PMF may show high ^{18}F -FDG uptake depending on the activity of inflammatory cells at the time of study.

In conclusion, ^{18}F -FDG PET can identify PMF mass lesions as hypermetabolic lesions even without associated lung malignancy or active tuberculosis. Therefore, ^{18}F -FDG PET might have a limited role in the diagnosis of PMF, particularly in the setting of PMF with possible superimposed inflammation or lung cancer.

References

1. Pathology standards for coal workers' pneumoconiosis. Report of the Pneumoconiosis Committee of the College of American Pathologists to the National Institute for Occupational Safety and Health. Arch Pathol Lab Med. 1979;103:375–432.
2. Spencer H. Pathology of the lung: the pneumoconiosis and other occupational lung diseases. Oxford: Pergamon; 1985. p. 413–510.
3. Williams JL, Moller GA. Solitary mass in the lungs of coal miners. Am J Roentgenol Radium Ther Nucl Med. 1973; 117:765–70.
4. Bergin CJ, Muller NL, Vedal S, Chan-Yeung M. CT in silicosis: correlation with plain films and pulmonary function tests. Am J Roentgenol. 1986;146:477–83.
5. Soutar CA, Collins HP. Classification of progressive massive fibrosis of coalminers by type of radiographic appearance. Br J Ind Med. 1984;41:334–9.
6. Nemery B. Metal toxicity and the respiratory tract. Eur Respir J. 1990;3:202–19.
7. Scatarige JC, Stitik FP. Induction of thoracic malignancy in inorganic dust pneumoconiosis. J Thorac Imaging. 1988;3:67–79.
8. Scarano D, Fadali AM, Lemole GM. Carcinoma of the lung and anthracosilicosis. Chest. 1972;62:251–4.
9. Dholakia S, Rappaport DC. The solitary pulmonary nodule. Is it malignant or benign? Postgrad Med. 1996;99:246–50.
10. Viggiano RW, Swensen SJ, Rosenow EC 3rd. Evaluation and management of solitary and multiple pulmonary nodules. Clin Chest Med. 1992;13:83–95.
11. Hustinx R, Benard F, Alavi A. Whole-body FDG-PET imaging in the management of patients with cancer. Semin Nucl Med. 2002;32:35–46.
12. Rohren EM, Turkington TG, Coleman RE. Clinical applications of PET in oncology. Radiology. 2004;231:305–32.
13. Bandoh S, Fujita J, Yamamoto Y, Nishiyama Y, Ueda Y, Tojo Y, et al. A case of lung cancer associated with pneumoconiosis diagnosed by fluorine-18 fluorodeoxyglucose positron emission tomography. Ann Nucl Med. 2003;17:597–600.
14. Je SK, Ahn MI, Park YH, Kim CH. Detection of a small lung cancer hidden in pneumoconiosis with progressive massive fibrosis using F-18 fluorodeoxyglucose PET/CT. Clin Nucl Med. 2007;32(3):247–8.
15. O'Connell M, Kennedy M. Progressive massive fibrosis secondary to pulmonary silicosis appearance on F-18 fluorodeoxyglucose PET/CT. Clin Nucl Med. 2004;29:754–5.
16. Kavanagh PV, Stevenson AW, Chen MY, Clark PB. Nonneoplastic diseases in the chest showing increased activity on FDG PET. AJR Am J Roentgenol. 2004;183:1133–41.
17. Jung JI, Park SH, Lee JM, Hahn ST, Kim KA. MR characteristics of progressive massive fibrosis. J Thorac Imaging. 2000;15:144–50.
18. McCloskey M, Cook N, Cameron D, Summers Q. Progressive massive fibrosis in the absence of lung nodulation. Australas Radiol. 1997;41:63–4.
19. Katabami M, Dosaka-Akita H, Honma K, Saitoh Y, Kimura K, Uchida Y, et al. Pneumoconiosis-related lung cancers: preferential occurrence from diffuse interstitial fibrosis-type pneumoconiosis. Am J Respir Crit Care Med. 2000;162:295–300.

20. Matsumoto S, Mori H, Miyake H, Yamada Y, Ueda S, Oga M, et al. MRI signal characteristics of progressive massive fibrosis in silicosis. *Clin Radiol*. 1998;53:510–4.
21. Matsumoto S, Miyake H, Oga M, Takaki H, Mori H. Diagnosis of lung cancer in a patient with pneumoconiosis and progressive massive fibrosis using MRI. *Eur Radiol*. 1998;8:615–7.
22. Alavi A, Gupta N, Alberini JL, Hickeson M, Adam LE, Bhargava P, et al. Positron emission tomography imaging in nonmalignant thoracic disorders. *Semin Nucl Med*. 2002;32:293–321.
23. Fraser R, Pare J. *Diagnosis of disease of the chest*. Philadelphia: Saunders; 1989. p. 2412–3.